Catalysis Today 183 (2012) 65–71

Contents lists available at ScienceDirect

Catalysis Today

journal homepage: www.elsevier.com/locate/cattod

Improved performance of magnetically recoverable Ce-promoted Ni/Al_2O_3 catalysts for aqueous-phase hydrogenolysis of sorbitol to glycols

Linmin Ye, Xinping Duan, Haiqiang Lin, Youzhu Yuan*

State Key Laboratory of Physical Chemistry of Solid Surfaces, National Engineering Laboratory for Green Chemical Productions of Alcohols–Ethers–Esters, College of Chemistry and Chemical Engineering, Xiamen University, Xiamen 361005, PR China

ARTICLE INFO

Article history:
Received 20 June 2011
Received in revised form 1 August 2011
Accepted 2 August 2011
Available online 31 August 2011

Keywords:
Ni/Al_2O_3
Cerium
Hydrogenolysis
Sorbitol
Glycols
Deactivation

ABSTRACT

The addition of cerium into Ni/Al_2O_3 catalysts afforded a remarkable promoting effect on catalytic performance of aqueous-phase hydrogenolysis of sorbitol to produce glycols (e.g., 1,2-propylene glycol and ethylene glycol). This effect was observed whether the catalysts were prepared through deposition–precipitation (DP) or co-precipitation (CP) methods. However, the $Ce–Ni/Al_2O_3$-DP catalyst went through rapid deactivation during the consecutive recycles. The $Ce–Ni/Al_2O_3$-CP catalyst was recovered easily by magnetic separation and reused over ten times. At a temperature of 513 K and pressure of 7.0 MPa, the $Ce–Ni/Al_2O_3$-CP catalyst maintained sorbitol conversion at above 90% and selectivity to glycols at 55–60% for 12 h. Characteristic studies indicate that the addition of cerium to the Ni/Al_2O_3 catalysts slightly lowered the reduction temperature of nickel oxide but considerably enhanced the H_2-chemisorption amount. Furthermore, the co-precipitation method was conducive for preparing the catalyst with high thermal stability, which was shown by 20% Ni/Al_2O_3-CP being more stable in structure than 20% Ni/Al_2O_3-DP under higher temperatures. The catalyst deactivation was due to the agglomeration of Ni nanoparticles during hydrogenolysis process in aqueous-phase.

1. Introduction

Sorbitol, which can be produced industrially in large amount by the hydrogenation of glucose over Raney Ni catalyst, is an important renewable carbon source and has been considered as one of the 12 top building blocks of biorefinery [1–5]. Glycols like ethylene glycol (EG), 1,2-propylene glycol (1,2-PG) and 1,3-propylene glycol (1,3-PG) are important chemicals traditionally produced by the petrochemical methods. Declining fossil fuel and increasing fossil fuel prices are pushing for the development of new economical process for the production of glycols. Nowadays, sorbitol is not only used as a sweetener in diet foods but also as a potential raw material for the synthesis of a variety of value-added chemicals, such as isosorbide, fuels, glycols and even hydrogen [6–9]. Hydrogenolysis of sorbitol may be an alternative method for producing glycols.

So far, conventional hydrogenation catalysts such as Ni, Ru, Pd and Pt have been employed for the hydrogenolysis of sorbitol to glycols. For example, the hydrogenolysis of a 5 wt% aqueous solution of sorbitol over a Pd/C catalyst can give 70% selectivity to glycols [10]. The Ru/C catalyst modified with tin obtains more than 60% selectivity to glycols at a high temperature using 32 wt% aqueous solution of sorbitol as feedstock [11]. Although the noble metal catalysts usually exhibit good selectivity to glycols, the conversion of sorbitol is moderate because they have weak capacity for C–C bond cleavage. In contrast, the Ni-based catalysts always reach full conversion, although the selectivity to glycols is less than 50% [12–15]. Recently, Banu et al. reported that 1,2-PG is the major product over Ni–NaY catalyst, whereas glycerol is the major product over Pt–NaY [16]. The difference in selectivity may be due to the modes of adsorption of sorbitol over the two metals. Mechanism studies on the hydrogenolysis of sorbitol have focused on the pathway of bond cleavage [17–19]. Wang et al. used 1,3-diols as model compounds to demonstrate that the existence of α-H or β-H is the essential condition for the dehydrogenation and dehydration steps [18]. Several studies have focused on the recyclability and deactivation mechanism of catalysts for hydrogenolysis. Chao et al. found that the deactivation of the supported Ni catalyst is due to the oxidation of Ni species in a fixed bed reactor; it can be regenerated by washing with water–methanol solution and then reduced by flowing hydrogen [20].

A number of previous reports show that cerium can work as an excellent promoter for hydrogenation reactions [21–24]. However, no study on the performance–structure correlation of Ce-promoted Ni catalysts has been published for the aqueous-phase hydrogenolysis of sorbitol to glycols. The current study aims to develop catalysts with improved catalytic activity and prolonged lifespan for the aqueous-phase hydrogenolysis of sorbitol to glycols. The supported nickel catalysts using cerium as a promoter were

* Corresponding author. Tel.: +86 592 2181659; fax: +86 592 2183047.
E-mail address: yzyuan@xmu.edu.cn (Y. Yuan).

0920-5861/$ – see front matter © 2011 Elsevier B.V. All rights reserved.
doi:10.1016/j.cattod.2011.08.006

prepared by deposition–precipitation (DP) and co-precipitation (CP) methods. The performances of the catalysts were correlated with their textural and structural properties characterized by various measurements. Furthermore, the reason for the catalyst deactivation was discussed.

2. Experiments

2.1. Catalyst preparation

All reagents were purchased from Sinopharm Chemical Regent Co., Ltd. and used without further purification. For the catalyst of Ce–Ni/Al_2O_3-DP, γ-Al_2O_3 was first suspended into the aqueous solution containing definite amounts of $Ni(NO_3)_2{\cdot}6H_2O$ and $Ce(NO_3)_3{\cdot}6H_2O$. Then, 5.0 mol/L $NH_3{\cdot}H_2O$ was gradually added until the pH value of the mixture reached 8.0; the mixture was further aged for 1 h. After filtration and washing with hot water, the obtained green solid was dried at 393 K overnight and finally calcined at 773 K for 2 h in air. The precursor was then reduced in 5% H_2–95% N_2 atmosphere at 773 K for 1 h. For the catalyst of Ce–Ni/Al_2O_3-CP, definite amounts of $Ni(NO_3)_2{\cdot}6H_2O$, $Ce(NO_3)_3{\cdot}6H_2O$, $Al_2(NO_3)_3{\cdot}9H_2O$ and urea were dissolved into water and heated up to 363 K for 24 h with vigorous stirring. After filtration and washing with hot water, the obtained green solid was dried at 393 K overnight and was finally calcined at 773 K for 2 h in air. The precursor was then reduced in 5% H_2–95% N_2 atmosphere at 1073 K for 1 h.

Typically, the nominal Ni loading was controlled at 20 wt% and 0.5 wt% for the Ce loading. The actual Ni content was determined by an inductively coupled plasma-atomic emission spectrometry (ICP-AES) using a Thermo Electron IRIS Intrepid II XSP.

2.2. Catalytic testing

The catalytic performance was examined in a 100 mL stainless steel autoclave equipped with a mechanical stirrer. A definite quantity of catalyst, $Ca(OH)_2$ and 30 wt% sorbitol aqueous solution was placed into the reactor. The autoclave was purged with hydrogen three times and was heated up to the desired temperature. After the reaction, the reactor was cooled to room temperature and decompressed. The gas phase products were detected by a gas chromatograph (with hydrogen as carrier gas) equipped with a Porapak Q column (3 m × 3 mm) and a thermal conductivity detector. The liquid phase products were detected by high-performance liquid chromatograph (Shimazu LC 20 AT, 5.0 mmol/L H_2SO_4 as flowing phase) equipped with a Shodex SH 1011 column (8 mm × 300 mm) and a refractive index detector. The major products of the reaction were EG, 1,2-PG, 1,2-butylene glycol (1,2-BG), glycerol (GLY), CH_4 and CO_2 (Scheme 1). Small amounts of other by-products, such as lactic acid and pentanediol, were detected. The products were verified using authentic samples and quantified by an external standard method. The total carbon balance of the reaction was about 85–95%. In this work, the glycols refer to the sum of EG, 1,2-PG and 1,2-BG. In the recycling process, the catalyst was separated from the reactant by an aid of magnet and then washed with deionized water for three times. After that the catalyst was used for next run.

2.3. Transmission electron microscopy (TEM)

TEM images were obtained on a JEM-2100 electron microscope operated at an acceleration voltage of 200 kV. Samples for TEM measurements were ultrasonically dispersed in ethanol. Drops of suspensions were deposited on a copper grid coated with carbon.

2.4. Scanning electron microscopy (SEM)

SEM images of the samples were obtained on a HITACHI S-4800 scanning microscope operated at an acceleration voltage of 200 kV. Prior to analysis, all the samples were coated with platinum in a sputter coating unit. The contents of surface elements were measured by energy dispersive spectrometer.

2.5. X-ray diffraction (XRD)

XRD patterns were performed using a PANAlytical X′pert Pro diffractometer equipped with a graphite monochrometer and Cu K_α radiation. The operation voltage was 40 kV, and the current was 30 mA. For *in situ* XRD measurement, a catalyst precursor was placed in a stainless steel holder and was covered with a beryllium plate having a thickness of 0.1 mm. Then a 5% H_2–95% N_2 mixture was introduced at a flow rate of 50 mL/min when raising the temperature at a rate of 10 K/min. The XRD patterns were collected after the samples reached the preset temperatures for 5 min. The diffraction pattern was identified by matching it with the reference pattern included in the JCPDS data base. The full width at half maximum of Ni(2 0 0) diffraction at $2\theta = 51.8^\circ$ was used to calculate the Ni crystallite size using the Scherrer equation to avoid the overlapping diffraction lines between Ni and Al_2O_3. The average Ni crystallite sizes of typical samples were further determined by TEM micrograph counting.

2.6. H_2-temperature-programmed reduction (H_2-TPR)

H_2-TPR profiles were measured in a fix bed continuous flow reactor connected to a Hiden Qic-20 mass spectrometer. In a typical measurement, the as-dried sample (10 mg) was pretreated in Ar atmosphere at 473 K for 1 h and then reduced in a mixture of 5% H_2–95% Ar at a flow rate of 30 mL/min and heating rate of 10 K/min. The amount of H_2 consumption was measured using the mass spectrometer.

2.7. Superconductivity quantum interference device

The magnetization curves for catalyst were measured at 300 K under a varying magnetic field of −1 to 1 T on a Quantum Design MPMS-XL-7 superconductivity quantum interference device (SQUID) magnetometer. The sample (20 mg) was put into a plastic tube for measurement.

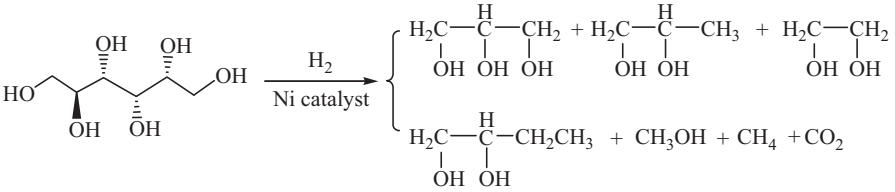

Scheme 1. Reaction products of catalytic hydrogenolysis of sorbitol over supported Ni catalyst in the aqueous phase.

2.8. Nitrogen adsorption–desorption

Nitrogen adsorption–desorption isotherms were measured by static N_2 physisorption at 77 K with a Micromeritics TriStar II 3020 surface area and pore analyzer. Before the N_2 physisorption measurement, all samples were outgassed at 393 K for 1 h and then evacuated at 573 K for 3 h to remove physically adsorbed impurities. The specific surface area (S_{BET}) was calculated by the Brunauer–Emmett–Teller method. The total pore volume (V_p) was derived from the adsorbed N_2 volume at a relative pressure of approximately 0.99. The Barrett–Joyner–Halenda method was used to calculate the pore size distributions according to the desorption branch of the isotherms.

2.9. Chemisorptions of CO and H_2

Ni dispersion was calculated according to the chemisorption of CO. The chemisorption of CO was performed using a Micromeritics ASAP 2020C. The sample was purged with high purity H_2 (99.999%) at 723 K for 30 min and then evacuated for 30 min. After cooling to 308 K under vacuum, CO was introduced, and the first isotherm (total CO uptake) was measured. After the first isotherm, the sample was evacuated for 10 min before the second isotherm (reversible CO uptake) was measured. The amount of chemisorbed CO was the difference between the total and the reversibly adsorbed CO. The chemisorption isotherms of H_2 were measured by similar procedures.

3. Results and discussion

3.1. Hydrogenolysis products of sorbitol over supported Ni catalysts

A preliminary experimental result showed that sorbitol was mainly converted into GLY, EG and 1,2-PG over several supported Ni catalysts as illustrated in Scheme 1. The selectivity to glycols can markedly be increased without decreasing sorbitol conversion when a base of $Ca(OH)_2$ is added [13]. A yield of glycols about 50% was obtained over the 20% Ni/Al_2O_3-DP catalyst with Ni nanoparticles (Ni NPs) of around 5 nm at 513 K, which is superior to other supported Ni catalysts investigated (Table S1).

Fig. 1 shows the reaction profile of the 20% Ni/Al_2O_3-DP catalyst as a function of reaction time at 493 K. The conversion increased linearly up to 100% when the reaction time was prolonged from 2 to 10 h. The selectivity to EG was constant throughout the reaction time investigated, whereas that to 1,2-PG increased and that to GLY decreased gradually. These results imply that the hydrogenolysis of sorbitol over the supported Ni catalyst was initiated most likely by the cleavage of C2–C3 bond between the second and third carbon atoms to generate GLY and EG as the primary products, 1,2-PG is essentially derived from GLY by the cleavage of the C–O bond in the first carbon atom.

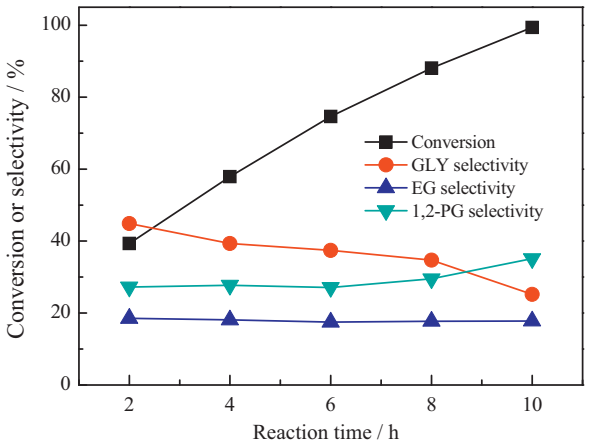

Fig. 1. Hydrogenolysis of sorbitol over 20% Ni/Al_2O_3-DP as a function of reaction time. Reaction conditions: sorbitol (30 wt% aqueous solution) = 20 mL; temp. = 493 K; P(H_2) = 7.0 MPa; catalyst weight = 0.80 g; $Ca(OH)_2$ = 0.10 g; stirring rate = 500 rpm.

3.2. Promotional effect of cerium

Table 1 lists the performance of cerium-promoted Ni/Al_2O_3-DP catalysts, with the cerium content ranging from 0.5% to 2%. For comparison, the reaction was carried out under lower temperature and shorter time. The conversion improved significantly with an increasing cerium loading. However, the product distributions were less sensitive to the cerium concentration under mild reaction conditions. When the reaction time was prolonged from 2 to 8 h, the catalyst with 2% Ce content resulted in 100% conversion of sorbitol. However, the outcome had lower selectivity to glycols and contained a large amount of gas phase products, namely CH_4 and CO_2. Since the catalysts can cause substantial reforming of sorbitol to give CO and H_2, and the CO undergoes shift to CO_2 and hydrogenation to CH_4, the increase of Ce species in the catalysts brought about not only the enhancement of activity but also the increase in the formation of gases such as CH_4 and CO. Nevertheless, the 0.5% Ce–20% Ni/Al_2O_3-DP catalyst could obtain a yield to glycols from 53–62% under a higher temperature and longer reaction time for the hydrogenolysis.

Table 2 compares the influences of Ni and Ce contents on the performance of the catalysts prepared through co-precipitation method. In agreement with the above results, the addition of cerium sharply accelerated the reaction rate of the Ni/Al_2O_3-CP catalysts at varying of Ni loadings. However, when the Ce-promoted

Table 1
Promotion effect of cerium on the hydrogenolysis of sorbitol to glycols over Ni/Al_2O_3-DP catalysts.

Catalyst	Conv. (%)	Selec.[a] (%)					
		GLY	EG	1,2-PG	1,2-BG	CH_4	CO_2
20% Ni/Al_2O_3-DP	39.3	44.9	18.5	27.2	1.5	3.2	3.1
0.5% Ce–20% Ni/Al_2O_3-DP	51.1	38.4	18.2	26.9	2.1	3.5	3.0
1% Ce–20% Ni/Al_2O_3-DP	65.0	36.6	18.2	24.7	1.8	2.2	1.8
2% Ce–20% Ni/Al_2O_3-DP	79.5	37.2	17.1	24.9	1.8	4.2	4.3
0.5% Ce–20% Ni/Al_2O_3-DP[b]	95.6	25.0	17.7	35.6	2.4	7.4	4.2
2% Ce–20% Ni/Al_2O_3-DP[b]	100.0	13.4	16.2	25.2	2.2	10.7	12.4
0.5% Ce–20% Ni/Al_2O_3-DP[c]	98.5	10.7	18.4	41.6	2.9	5.6	4.7

Reaction conditions: sorbitol (30 wt% aqueous solution) = 20 mL; temp. = 493 K; time = 2 h; P(H_2) = 7.0 MPa; catalyst weight = 0.80 g; $Ca(OH)_2$ = 0.10 g; stirring rate = 500 rpm.
[a] Others include lactic acid, pentanediol, several kinds of polyols and unknown compounds.
[b] Time = 8 h, others are the same as above.
[c] Temp. = 513 K, time = 8 h, others are the same as above.

Table 2
Promotion effect of cerium on the hydrogenolysis of sorbitol to glycols over Ni/Al_2O_3-CP catalysts.

Catalyst	Conv. (%)	Selec.[a] (%)					
		GLY	EG	1,2-PG	1,2-BG	CH_4	CO_2
10% Ni/Al_2O_3-CP	15.3	17.1	21.3	34.0	0	8.3	4.2
20% Ni/Al_2O_3-CP	41.8	14.0	20.0	35.6	2.3	8.7	3.3
30% Ni/Al_2O_3-CP	83.6	14.9	16.9	33.6	0.8	7.4	2.1
0.5% Ce–10% Ni/Al_2O_3-CP	41.3	9.4	20.4	34.9	2.3	7.3	3.8
0.5% Ce–20% Ni/Al_2O_3-CP	91.1	10.3	17.9	35.3	2.4	8.5	1.3
0.5% Ce–30% Ni/Al_2O_3-CP	99.8	2.4	7.1	25.5	2.3	17.0	5.6

Reaction conditions: sorbitol (30 wt% aqueous solution) = 20 mL; temp. = 513 K; time = 8 h; $P(H_2)$ = 7.0 MPa; catalyst weight = 0.80 g; $Ca(OH)_2$ = 0.10 g; stirring rate = 500 rpm.
[a] Others include lactic acid, pentanediol, several kinds of polyols and unknown compounds.

catalyst had a Ni loading higher than 20 wt%, lower selectivity to glycols and higher amounts of CH_4 and CO_2 were obtained.

3.3. Catalyst recycling

Fig. 2 shows the recycling results of 0.5% Ce–20% Ni/Al_2O_3-DP and 0.5% Ce–20% Ni/Al_2O_3-CP catalysts. The 0.5% Ce–20% Ni/Al_2O_3-DP catalyst could give a conversion up to 98% with selectivity to glycols of 62% in the first run. However, its catalytic activity and selectivity to glycols decreased rapidly after three runs. This finding indicates that the catalyst prepared by the deposition–precipitation method showed unsatisfactory stability in the aqueous-phase hydrogenolysis of sorbitol. In contrast, the 0.5% Ce–20% Ni/Al_2O_3-CP catalyst presented a promising result in the recycling process. As shown in Fig. 2, the sorbitol conversion reached 94% when the reaction time was prolonged to 12 h and the conversion was maintained up to 90% in 10 runs of recycling. The overall selectivity to glycols was also sustained at around 55–60%. Moreover, the catalyst could easily be recovered by magnetic separation in a few minutes and then be reused without significantly affecting their catalytic performance. After 11 runs, the conversion dropped to 86%, but it recovered to the original level when the fresh catalyst in about 12.5% of catalyst weight was replenished.

The Ni content in the aqueous phase was checked after each recycling by ICP-AES measurement. The results show that less than 0.06 wt% Ni was leach out from the fresh Ni catalyst in the first run and lower than 0.02 wt% Ni was lost in the following consecutive each recycling. Negligible conversion of sorbitol was obtained with such amount of Ni under the present reaction conditions. Therefore, the results imply that the different behaviors of 0.5% Ce–20% Ni/Al_2O_3-DP and 0.5% Ce–20% Ni/Al_2O_3-CP catalysts during the recycling periods were not related to the Ni leaching.

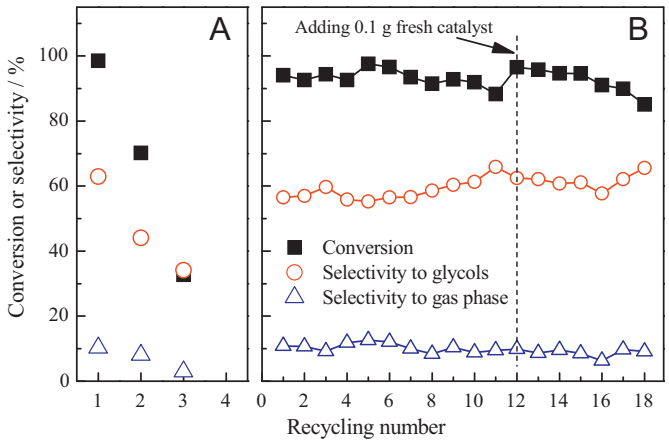

Fig. 2. Recycling of (A) 0.5% Ce–20% Ni/Al_2O_3-DP and (B) 0.5% Ce–20% Ni/Al_2O_3-CP catalysts for the hydrogenolysis of sorbitol. Reaction conditions: sorbitol (30 wt% aqueous solution) = 20 mL; temp. = 513 K; time = 8 h for 0.5% Ce–20% Ni/Al_2O_3-DP and 12 h for 0.5% Ce–20% Ni/Al_2O_3-CP; $P(H_2)$ = 7.0 MPa; catalyst weight = 0.80 g; $Ca(OH)_2$ = 0.10 g; stirring rate = 500 rpm.

3.4. Characterization

Table S2 gives the BET surface area (S_{BET}), pore volume (V_p) and average pore diameter (D_p) of supported Ni catalysts. Based on the results, the addition of cerium did not change the textual structure of the catalyst. The SEM images in Fig. S1 show that the supported Ni catalysts were porous materials. The surface Ni content in the 20% Ni/Al_2O_3-CP catalyst by energy dispersive X-ray spectroscopy (EDX) was less than the loading amount and was lower than that in the 20% Ni/Al_2O_3-DP one (Tables S2 and S3, and Fig. S2), suggesting that Ni NPs embedded into the Al_2O_3 matrix by the co-precipitation method. Data on Ni dispersion supported this viewpoint, *i.e.*, the 20% Ni/Al_2O_3-DP showed a Ni dispersion of 20.1%, whereas 20% Ni/Al_2O_3-CP showed a Ni dispersion of 2.9%. The magnetic curves of Ni/Al_2O_3 catalysts were evaluated by SQUID measurement (Fig. S3). The coercive force, which is symbolized as *M*, denotes the magnetism of materials. The *M* value of Ni/Al_2O_3-CP was 3.6 emu/g, which is much stronger than that of Ni/Al_2O_3-DP. The differences in magnetism may be related to their different particle sizes. Nonetheless, an alternative method for the separation of solid catalyst through the aid of a magnet was provided in the case of Ni/Al_2O_3-CP catalyst system.

Fig. 3 displays the H_2-TPR patterns of supported Ni catalyst precursors. The Ni content was maintained at 20% in each catalyst. The bulk NiO sample (Fig. 3A, curve a) produced two neighboring peaks at about 600 K, which is probably due to the different Ni particle size in this sample [25]. The reduction temperature became higher when the Ni species was immobilized on Al_2O_3, indicating the interactions between Ni species and support. The reduction behaviors between the samples with and without cerium were similar to each other, but the temperature gradually decreased with the increase in cerium amount from 0.5 to 2%. The H_2-TPR profiles of 20% Ni/Al_2O_3-CP and 0.5% Ce–20% Ni/Al_2O_3-CP in Fig. 3B show little differences between catalysts with or without a cerium promoter. In comparison with 20% Ni/Al_2O_3-DP catalyst, the 20% Ni/Al_2O_3-CP one presented a broad reduction peak ranging from 800 to 1100 K, suggesting that there were stronger interactions between Ni species and Al_2O_3 compared with Ni/Al_2O_3-DP.

Fig. 4 illustrates the *in situ* XRD patterns of the above two types of catalysts as a function of reduction temperature under an atmosphere of 5%H_2–95%Ar. The diffraction lines at 44.5°, 51.8°, and 76.3° were attributed to the Ni(1 1 1), Ni(2 0 0) and Ni(2 2 0) crystal planes, respectively. The Ni(2 0 0) diffraction line of 20% Ni/Al_2O_3-DP appeared at 923 K. This diffraction line enhanced sharply when reduction temperature was further increased. The co-precipitation method was conductive for preparing the catalyst with high thermal stability, which is shown by 20% Ni/Al_2O_3-CP being more stable than 20% Ni/Al_2O_3-DP at higher temperatures. Figs. 5 and 6 show the XRD patterns and the TEM images of the Ce-promoted catalysts

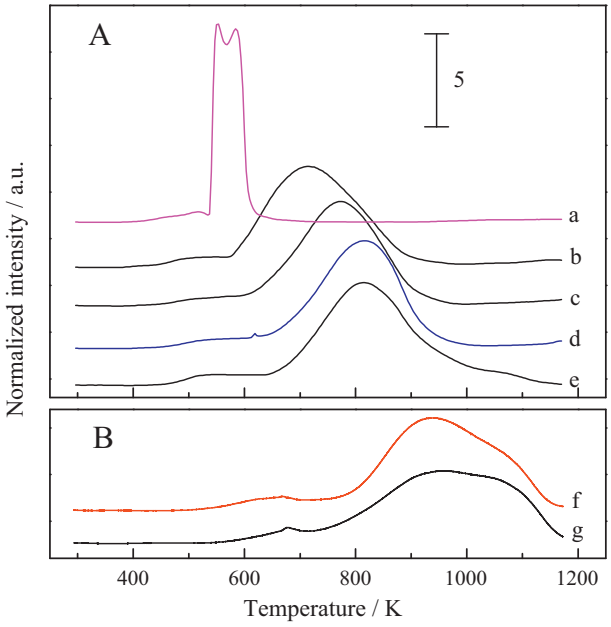

Fig. 3. H_2-TPR profiles of as-calcined (A) Ce–Ni/Al_2O_3-DP and (B) Ce–Ni/Al_2O_3-CP samples. (a) NiO; (b) 2% Ce–20% Ni/Al_2O_3-DP; (c) 1% Ce–20% Ni/Al_2O_3-DP; (d) 0.5% Ce–20% Ni/Al_2O_3-DP; (e) 20% Ni/Al_2O_3-DP; (f) 0.5% Ce–20% Ni/Al_2O_3-CP and (g) 20% Ni/Al_2O_3-CP.

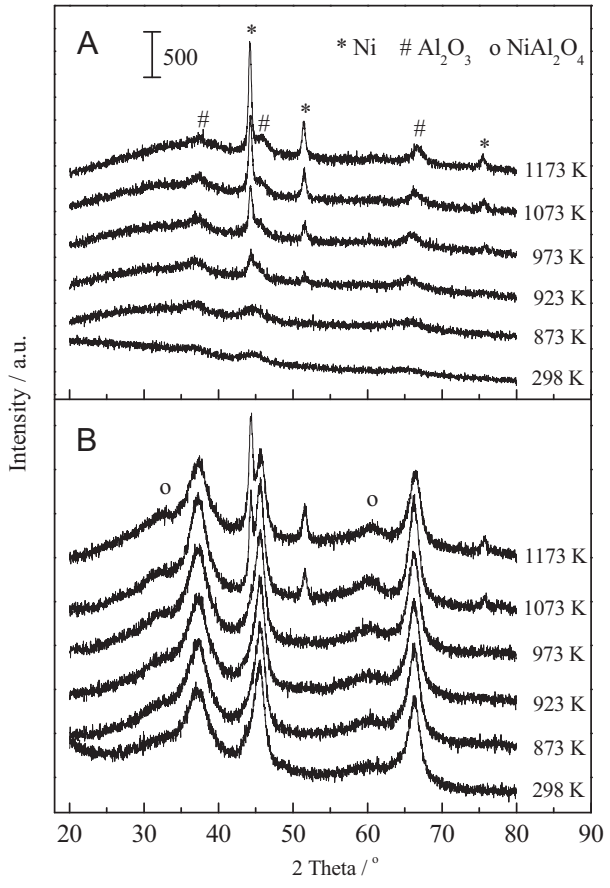

Fig. 4. *In situ* XRD patterns of (A) 20% Ni/Al_2O_3-DP and (B) 20% Ni/Al_2O_3-CP as a function of reduction temperature under an atmosphere of 5%H_2–95%Ar.

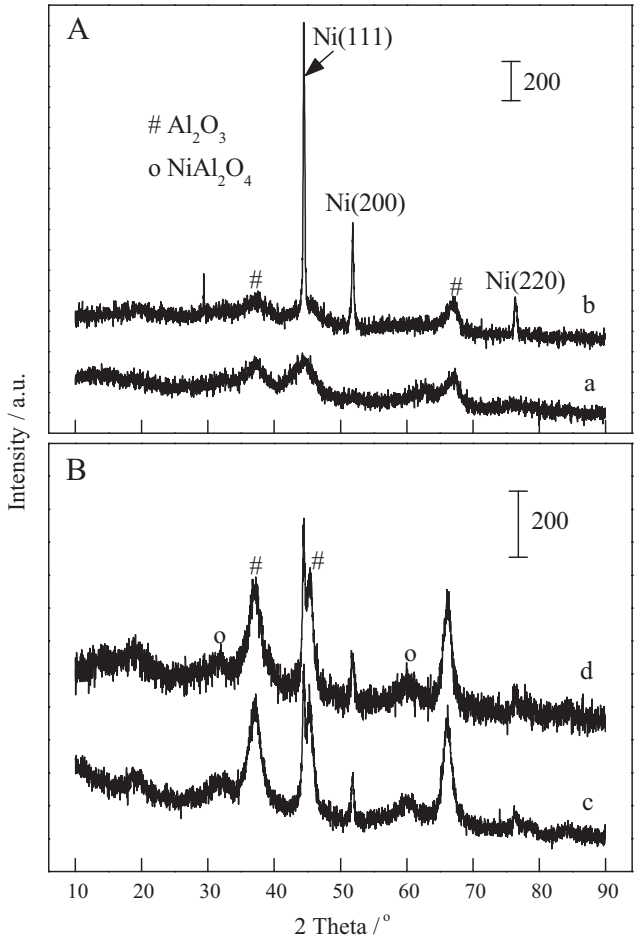

Fig. 5. XRD patterns of (A) 0.5% Ce–20% Ni/Al_2O_3-DP and (B) 0.5% Ce–20% Ni/Al_2O_3-CP before and after reaction. (a) As-reduced 0.5% Ce–20% Ni/Al_2O_3-DP; (b) 0.5% Ce–20% Ni/Al_2O_3-DP after three recyclings; (c) as-reduced 0.5% Ce–20% Ni/Al_2O_3-CP and (d) 0.5% Ce–20% Ni/Al_2O_3-CP after eighteen recyclings.

before and after the reaction. Without Ce, the average size of Ni NPs was around 5.1 nm in the 20% Ni/Al_2O_3-DP catalyst (Table S1), but if Ce was involved, it decreased to 2.9 nm in the 20% Ce–Ni/Al_2O_3-DP one (Figs. 5A-a and 6a). The particle size increased drastically to around 89.6 nm after the third run (Figs. 5A-b and 6b), indicating that a significant agglomeration of Ni NPs occurred in the case of 0.5% Ce–20% Ni/Al_2O_3-DP catalyst during the reaction. As for the 0.5% Ce–20% Ni/Al_2O_3-CP catalyst, however, there were slight differences in the XRD patterns (Fig. 5B) and TEM images (Fig. 6, images c and d) between the fresh catalyst and the one after eighteen runs, indicating that the Ni NPs mostly maintained their sizes during the recycles. Therefore, the co-precipitation method was beneficial because it could enhance the interaction between Ni NPs and support. Given the results, the agglomeration of Ni NPs was determined as the main reason for deactivation, it could be depressed by enhancing the interaction between metal and support.

The function of Ce species for improving the catalytic activity has mainly been ascribed to the electron effect of Ce-ions in literature [21–24]. That is, the presence of Ce^{4+}/Ce^{3+} species in the catalyst is beneficial for adjusting the electron density of metallic Ni and thus improving the reaction activity. When the 2% Ce–20% Ni/Al_2O_3-DP catalyst was employed, it exhibited an improved catalytic performance as compared with 20% Ni/Al_2O_3-DP under identical conditions (Table 1). Nonetheless, the average size of Ni NPs was decreased from 5.1 to 2.9 nm when Ce was introduced

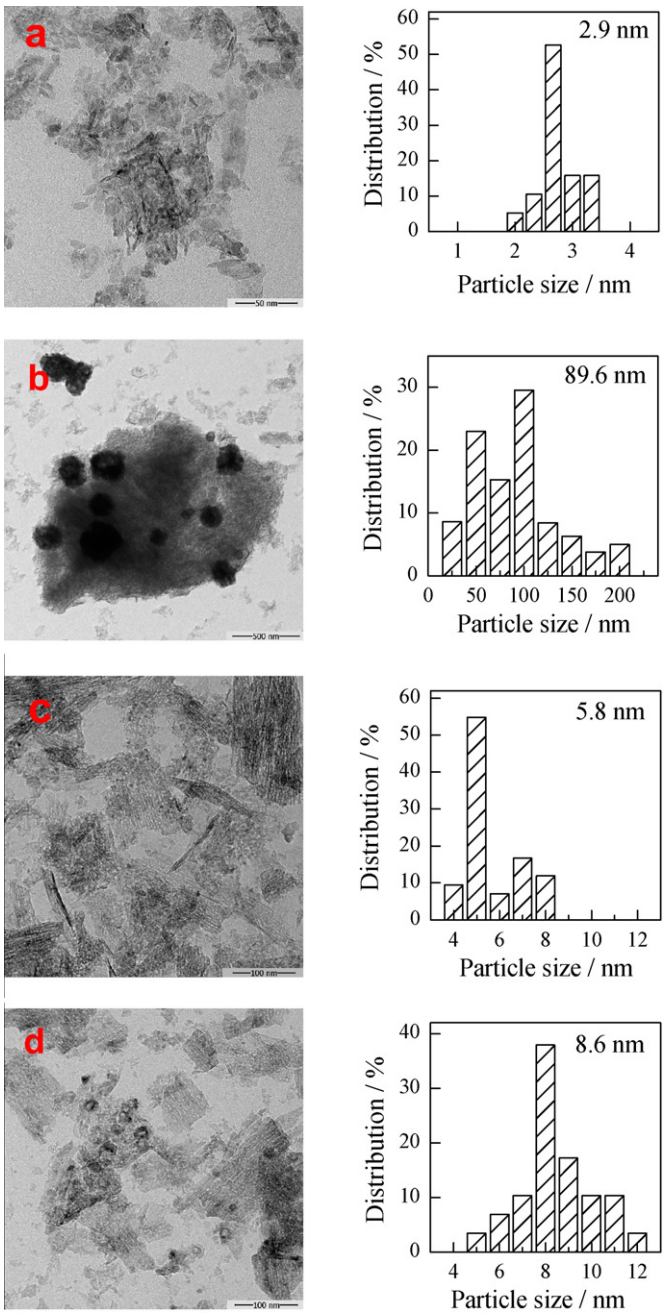

Fig. 6. TEM images of Ce–Ni/Al_2O_3 catalysts before and after reaction. (a) As-reduced 0.5% Ce–20% Ni/Al_2O_3-DP; (b) 0.5% Ce–20% Ni/Al_2O_3-DP after three recyclings; (c) as-reduced 0.5% Ce–20% Ni/Al_2O_3-CP; (d) 0.5% Ce–20% Ni/Al_2O_3-CP after eighteen recyclings.

(Table S1). A smaller Ni particle is believably able to provide more active sites for the adsorption of H_2, leading to a higher hydrogenolysis activity. To obtain an insight into the performance of cerium, H_2-chemisorption was measured for the Ni/Al_2O_3 catalysts with and without cerium. Fig. 7 shows that the addition of cerium into the Ni/Al_2O_3 catalysts greatly enhanced the chemisorption amount of H_2. These adsorbed hydrogen species may be activated by Ni NPs and thus contribute to the hydrogenolysis of sorbitol. Thus, the electron effect of Ce-ions and the decreased size of Ni NPs could not be excluded to be responsible for the increase of H_2 adsorption and the enhancement of activity in the presence of Ce. However, a proper amount of cerium additive was required for adjusting the activity and selectivity to achieve higher performance.

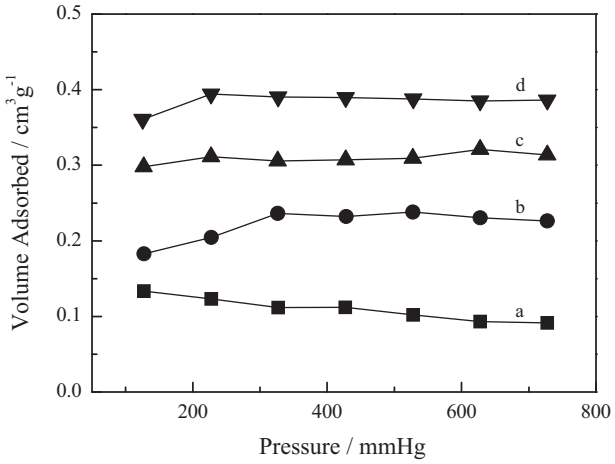

Fig. 7. H_2-chemisorption isotherm profiles of as-reduced catalysts. (a) 20% Ni/Al_2O_3-DP; (b) 0.5% Ce–20% Ni/Al_2O_3-DP; (c) 1% Ce–20% Ni/Al_2O_3-DP and (d) 2% Ce–20% Ni/Al_2O_3-DP.

4. Conclusion

Cerium is an efficient promoter to improve the performance of Ni/Al_2O_3 catalysts for the aqueous-phase hydrogenolysis of sorbitol to glycols. The optimal loadings of Ni and Ce were about 20% and 0.5%, respectively. The enhanced effect was related to the increase in chemisorption amount of H_2 on the Ce-containing catalysts. The catalyst deactivation was mainly attributed to the agglomeration of Ni NPs during the reaction process. Methods that can enhance the dispersion and improve the stability of Ni NPs can be beneficial for the preparation of highly efficient catalysts.

The 0.5% Ce–20% Ni/Al_2O_3-CP catalyst with a mean particle size of around 5 nm showed good activity, high selectivity to glycols and superior recyclability. The catalyst was easily separated from the aqueous-phase reactant with the aid of magnet and was reused many times with a negligible drop in its hydrogenolysis performance. The sorbitol conversion reached above 90% and the overall selectivity to glycols was sustained at 55–60% during the eighteen recyclings at 513 K under 7.0 MPa for 12 h.

Acknowledgements

We acknowledge the financial supports provided by the National Basic Research Program of China (No. 2011CBA00508), the National Natural Science Foundation of China (Nos. 20873108 and 20923004), and the Key Scientific Project of Fujian Province (No. 2009HZ0002-1).

Appendix A. Supplementary data

Supplementary data associated with this article can be found, in the online version, at doi:10.1016/j.cattod.2011.08.006.

References

[1] S. Fernando, S. Adhikari, C. Chandrapal, N. Murali, Energy Fuels 20 (2006) 1727.
[2] P. Gallezot, P.J. Cerino, B. Blanc, G. Flèche, P. Fuertes, J. Catal. 146 (1994) 93.
[3] B.W. Hoffer, E. Crezee, F. Devred, P.R.M. Mooijman, W.G. Sloof, P.J. Kooyman, A.D. van Langeveld, F. Kapteijn, J.A. Moulijn, Appl. Catal. A: Gen. 253 (2003) 437.
[4] B. Kusserow, S. Schimpf, P. Claus, Adv. Syn. Catal. 345 (2003) 289.
[5] M.C.M. Castoldi, L.D.T. Câmara, R.S. Monteiro, A.M. Constantino, L. Camacho, J.W.M. de Carneiro, D.A.G. Aranda, React. Kinet. Catal. Lett. 91 (2007) 341.
[6] G.W. Huber, J.W. Shabaker, J.A. Dumesic, Science 300 (2003) 2075.
[7] J.N. Chheda, G.W. Huber, J.A. Dumesic, Angew. Chem. Int. Ed. 46 (2007) 7164.
[8] P.L. Dhepe, A. Fukuoka, Catal. Surv. Asia 11 (2007) 186.
[9] E.L. Kunkes, D.A. Simonetti, R.M. West, J.C. Serrano-Ruiz, C.A. Gärtner, J.A. Dumesic, Science 322 (2008) 417.

[10] B.W. Hoffer, R. Prochazka, US 2010/0019191 A1, 2010.
[11] G. Gubitosa, B. Casale, US 5403805, 1995.
[12] H.S. Rothrock, US 2004135, 1935.
[13] I.T. Clark, Ind. Eng. Chem. 50 (1958) 1125.
[14] T.A. Werpy, J.G. Frye, A.H. Zacher, D.J. Miller, US 2003/0119952 A1, 2003.
[15] J. Liu, J. Xu, CN 101199930A, 2008.
[16] M. Banu, S. Sivasanker, T.M. Sankaranarayanan, P. Venuvanalingam, Catal. Commun. 12 (2011) 673.
[17] D.K. Sohounloue, C. Montassier, J. Barbier, React. Kinet. Catal. Lett. 22 (1983) 391.
[18] K.Y. Wang, M.C. Hawley, T.D. Furney, Ind. Eng. Chem. Res. 34 (1995) 3766.
[19] N. Li, G.W. Huber, J. Catal. 270 (2010) 48.
[20] J.C. Chao, D.T.A. Huiber, US 4366332, 1982.
[21] R.L. Manfro, A.F. da Costa, N.F.P. Ribeiro, M.M.V.M. Souza, Fuel Process. Technol. 92 (2011) 330.
[22] W.Q. Wang, J. Zhao, H. Ma, H. Miao, Q. Song, J. Xu, Appl. Catal. A: Gen. 383 (2010) 73.
[23] J.L. Liu, L.J. Zhu, Y. Pei, J.H. Zhuang, H. Li, H.X. Li, M.H. Qiao, K.N. Fan, Appl. Catal. A: Gen. 353 (2009) 282–287.
[24] A. Sepúlveda-Escribano, F. Coloma, F. Rodríguez-Reinoso, J. Catal. 178 (1998) 649–657.
[25] Ch.P. Li, Y.W. Chen, Thermochim. Acta 256 (1995) 457.